Available online at www.sciencedirect.com
SCIENCE DIRECT®
International Journal of Heat and Fluid Flow 25 (2004) 741–748
International Journal of HEAT AND FLUID FLOW
www.elsevier.com/locate/ijhff

Unsteady heat transfer from a circular cylinder for Reynolds numbers from 3000 to 15,000

Hajime Nakamura *, Tamotsu Igarashi

Department of Mechanical Engineering, National Defense Academy, 1-10-20 Hashirimizu, Yokosuka, Kanagawa 239-8686, Japan

Received 9 January 2004; accepted 12 May 2004
Available online 7 July 2004

Abstract

Unsteady heat transfer from a circular cylinder to the cross-flow of air was investigated experimentally for Reynolds numbers from 3000 to 15,000. Fluctuating heat transfer on the cylinder surface was measured using a heat flux sensor, and time-spatial characteristics of the heat transfer were measured using an infrared thermograph. The present measurements showed that the alternating rolling-up of the shear layers that separated from the cylinder forms an alternating reattached flow at the rear of the cylinder in the range of $Re > 5000$–8000, due to the forward movement of the vortex formation region with increasing Reynolds number. This leads to a sharp increase in the time-averaged Nusselt number around the rear stagnation point of the cylinder. The heat transfer in the separated flow region has spanwise nonuniformity throughout the examined Reynolds number range. The wavelength of this nonuniformity corresponds to that of the streamwise vortices formed in the near-wake.

Keywords: Forced convection; Unsteady heat transfer; Circular cylinder; Separated flow; Reynolds number

1. Introduction

The Nusselt number in the separated flow on the rear of two-dimensional bluff bodies is proportional to the 2/3 power of Reynolds number in the range of $Re = 10^4$–10^5, according to Richardson (1963), and Igarashi and Hirata (1977). However, this correlation is not valid for lower Reynolds numbers, $Re < 1.5 \times 10^4$ for a circular cylinder, contradictory to the expectation by Richardson (1963). Fig. 1 shows the latest results for the Nusselt number at the rear stagnation point of a circular cylinder obtained by Nakamura and Igarashi (2002b). This Figure clearly shows a departure from the correlation of the 2/3 power below $Re = 1.5 \times 10^4$. Interestingly, this trend, having a lobe at around $Re = 200$ and a dip at around $Re = 1500$–3000, is strongly correlated to the flow behind a circular cylinder, with respect to, for example, base pressure coefficient (Roshko, 1993; Williamson, 1996a, among others) and vortex formation length (Bloor, 1964, Nakamura and Igarashi, 2002b, among others).

Notably, the Nusselt number increases sharply in the range of $3000 < Re < 15,000$ with increasing the Reynolds number, as shown in Fig. 1. Fluctuating lift and sound pressure also increase suddenly in this Reynolds number range (Norberg, 2003, among others). A remarkable change in the flow in this regime was first investigated by Schiller and Linke (1933), who reported a sharp decrease in the base pressure coefficient at the rear of the cylinder with the shortening of the recirculating region behind the cylinder. This change originates from the forward movement of the "turbulent-transition point" in the separated shear layers caused by Kelvin–Helmholtz instability. In addition, the other transition occurs in the near-wake at around $Re = 5000$, as suggested by Norberg (1993). This transition is confirmed to be caused by vortex dislocations along the span (Prasad and Williamson, 1997), although the origin of this transition remains unclear.

An investigation of unsteady heat transfer is very helpful to clarify the flow in the vicinity of the body

* Corresponding author. Tel.: +81-46-841-3810; fax: +81-468-44-5900.
E-mail address: nhajime@nda.ac.jp (H. Nakamura).

0142-727X/$ - see front matter © 2004 Elsevier Inc. All rights reserved.
doi:10.1016/j.ijheatfluidflow.2004.05.012

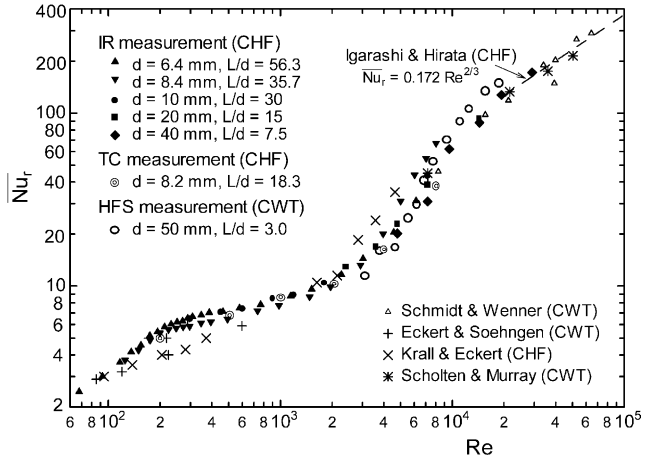

Fig. 1. Nusselt number at the rear stagnation point of a circular cylinder.

surface, because the unsteady heat transfer reflects the characteristics of the flow near the surface. Several attempts have been made to measure the unsteady heat transfer in the separated flow region of the cylinder (Peterka and Richardson (1969) for $Re = 5500$–$10,900$, Boulos and Pei (1974) for $Re = 3000$–9000, Kumada et al. (1992) at around $Re = 30,000$, Scholten and Murray (1998) for $Re = 7000$–$50,000$ and Nakamura and Igarashi (2002a) at around $Re = 20,000$). However, the findings reported by Peterka and Richardson (1969) and Boulos and Pei (1974) were not complete because of both the one-point measurement and the inadequate response time of the heat-flux sensor used in their studies. Other studies have focused on heat transfer in the range of $Re > 10^4$, in which the 2/3 power law is satisfied.

Recently, Nakamura and Igarashi (2003) reported an investigation of the unsteady and three-dimensional characteristics of the heat transfer at the rear of the cylinder over a wide range of Reynolds numbers from $Re = 120$ to 30,000. In the present paper, a drastic change in the heat transfer in the range of $3000 < Re < 15,000$ is investigated.

2. Experimental apparatus and procedure

Fluctuating heat transfer was measured using a heat flux sensor. Fig. 2(a) shows a schematic diagram of a circular cylinder having a diameter of $d = 50$ mm and a length of $L = 150$ mm, which was set horizontally in a wind tunnel. The freestream velocity ranged from 1 to 6

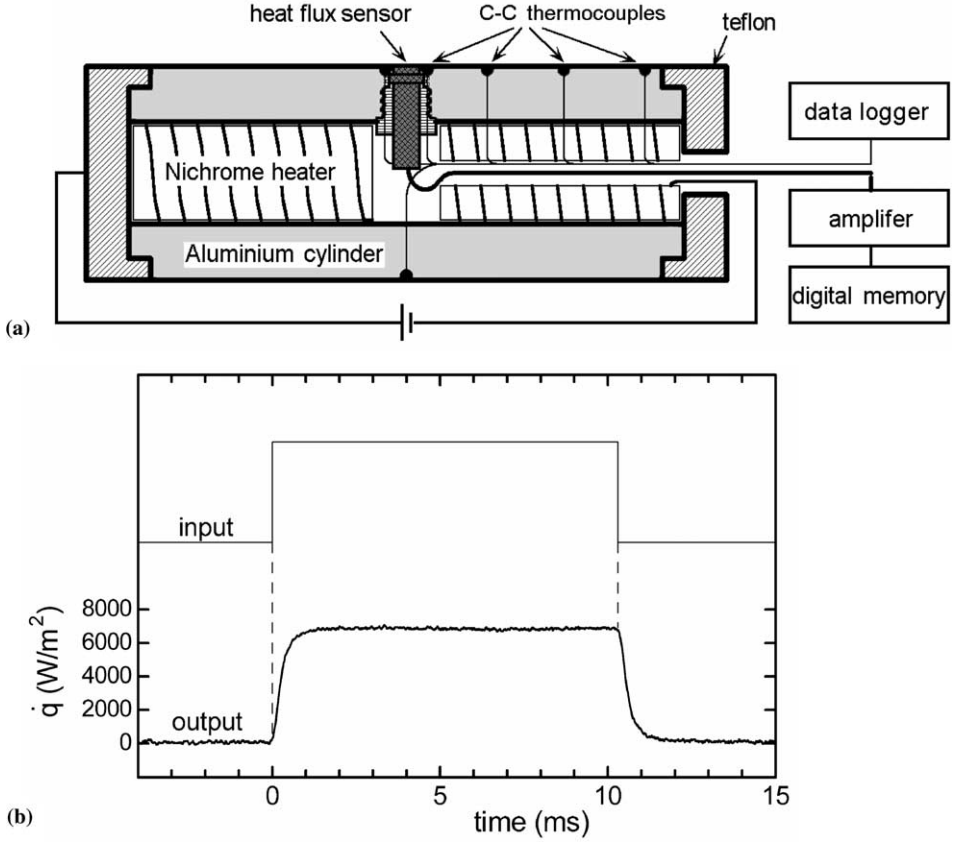

Fig. 2. Test model for measurement of fluctuating heat transfer: (a) schematic diagram of circular cylinder and (b) time response of heat flux sensor.

m/s, resulting in Reynolds numbers, based on d, ranging from $Re = 3000$ to 18,900. The cylinder was heated under the condition of constant wall temperature. The temperature difference between the heated surface and the freestream was approximately 25 °C. The effect of natural convection was insignificant under the present experimental conditions. A heat flux sensor (HFM-7E/L, Vatell) was attached at the center of the cylinder axis. The heat transfer coefficient measured by the sensor was evaluated taking into account radiative heat flux.

Fig. 2(b) shows the time response of the heat flux sensor to a stepwise change. The input signal was generated by the radiation from a halogen lamp, intercepted intermittently by a chopper. The time constant of the sensor was evaluated to be 0.3 ms, which was determined by extrapolating an exponential curve to the delayed signal. Since the output signal almost reaches to an asymptotic value at 2 ms after the stepwise change, the attenuation of the fluctuation is negligible up to 500 Hz, which was much faster than the vortex shedding frequency behind the cylinder (~25 Hz).

Time-spatial characteristics of the heat transfer were measured via infrared thermography. Fig. 3(a) shows a schematic diagram of the test cylinder, having a diameter of $d = 40$ mm and a length of $L = 300$ mm, which was set horizontally in a wind tunnel. The freestream velocity ranged from 2 to 4 m/s, resulting in Reynolds numbers, based on d, ranging from $Re = 4800$ to 9600. The test cylinder has a 200-mm-long semi-circular section removed from its center. A sheet of stainless-steel foil of 0.01 mm in thickness covered the cylinder surface, including the removed section. The surface of the cylinder was heated by applying a direct current to the stainless-steel foil under the condition of constant heat flux. The temperature difference between the heated surface and the freestream was 10–30 °C. The surface of the cylinder was coated using black paint in order to enhance the emissivity of the infrared radiation. The infrared thermograph was positioned downstream from the circular cylinder, as shown in Fig. 3(b), and was used to measure temperature distributions on the cylinder surface. The infrared thermograph used in the present study (TVS-8502, Avio) can capture images of instantaneous temperature distribution at 120 frames per second, and a total of 1024 frames with a full resolution of 256×236 pixels. The heat transfer coefficient measured by the infrared thermograph was evaluated taking into account radiative heat flux and heat conduction losses, as described in detail by Nakamura and Igarashi (2002b, 2003).

The time response of temperature on a thin wall, assuming the radiative heat flux and heat conduction losses are small, can be expressed as follows:

$$c\rho\delta\frac{\mathrm{d}T_w}{\mathrm{d}t} = \dot{q}_{in} - h(T_w - T_0), \tag{1}$$

where c, ρ and δ are specific heat, density and thickness of the wall, respectively, T_w and T_0 are wall and free-stream temperatures, respectively, $\dot{q}_{in}$ is input heat flux to the wall, and h is heat transfer coefficient from the heated wall. Then, the time constant is defined as

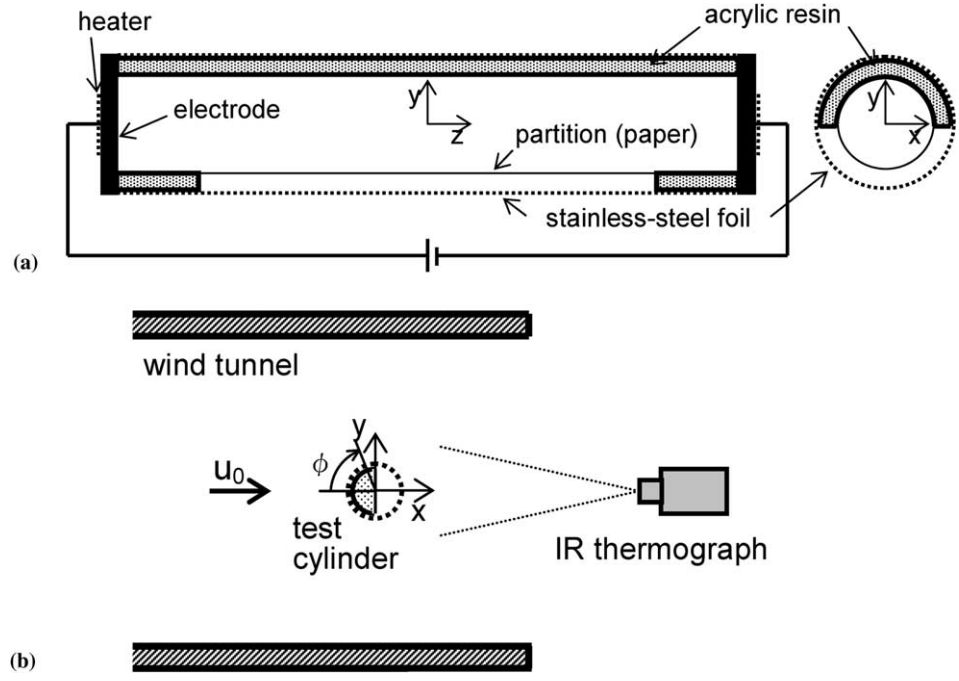

Fig. 3. Test model for measurement of time-spatial characteristics of heat transfer: (a) schematic diagram of circular cylinder and (b) location of infrared thermograph.

$$\tau = c\rho\delta/h. \quad (2)$$

This implies that the time constant is proportional to the heat capacity of the wall and inversely proportional to the heat transfer coefficient. In order to obtain the value of $c\rho\delta$ for the infrared measurements, the time constant of the wall, which was fabricated from 0.01 mm thick stainless-steel foil coated with black paint, was evaluated experimentally. This was performed in a steady flow condition of a laminar boundary layer formed on a flat plate. The delayed signal of T_w was obtained to a stepwise change of the direct current applied to the foil. The time constant was evaluated to be $\tau = 1.5$–3 second in the range of the heat transfer coefficient for the cylinder experiments ($h = 20 - 40$ W/m^2 K). This indicates that the fluctuation of the heat transfer for the infrared measurements was considerably attenuated at the vortex shedding frequency (10–20 Hz). However, the fluctuation was observable because the resolution of the temperature for the infrared measurements was small enough (0.025 °C) compared to the temperature difference between the heated wall and the free-stream (10–30 °C).

3. Fluctuating heat transfer

3.1. Nusselt number distribution

Fig. 4(a) and (b) show the distributions of time-averaged Nusselt number, $\overline{Nu}/Re^{0.5}$, and the r.m.s. value of the fluctuating Nusselt number $\sqrt{Nu'^2}/Re^{0.5}$, respectively, as measured by the heat flux sensor under the condition of constant wall temperature. In the laminar flow region ($\phi < 80°$), the distribution of time-averaged Nusselt number agrees well with that obtained by Schmidt and Wenner (1941), and the value of fluctuating Nusselt number is very low in the region of $\phi < 60°$, in which ϕ reflects the angle from the front stagnation point of the cylinder. At approximately $\phi = 70°$–$80°$, a hump appears in the fluctuating Nusselt number, probably due to an effect of the fluctuation of the separated shear layer. This is particularly apparent for the higher Reynolds numbers ($Re > 7000$). In the separated flow region ($\phi > 90$–$100°$), the value of $\sqrt{Nu'^2}$ is very-high, approximately half the value of $\overline{Nu}$, corresponding to that for the higher Reynolds number ($Re \approx 20,000$, Nakamura and Igarashi, 2002a). The distribution of the fluctuating Nusselt number in the separated flow region has a similar feature to that of the time-averaged Nusselt number, which increases toward the rear stagnation point ($\phi = 180°$). It should be noted that both distributions of time-averaged and fluctuating Nusselt numbers have a plateau in the region of $110° \leqslant \phi \leqslant 130°$ for higher Reynolds numbers ($Re > 7000$). This indicates a change in the flow pattern at around $Re = 7000$, as described later.

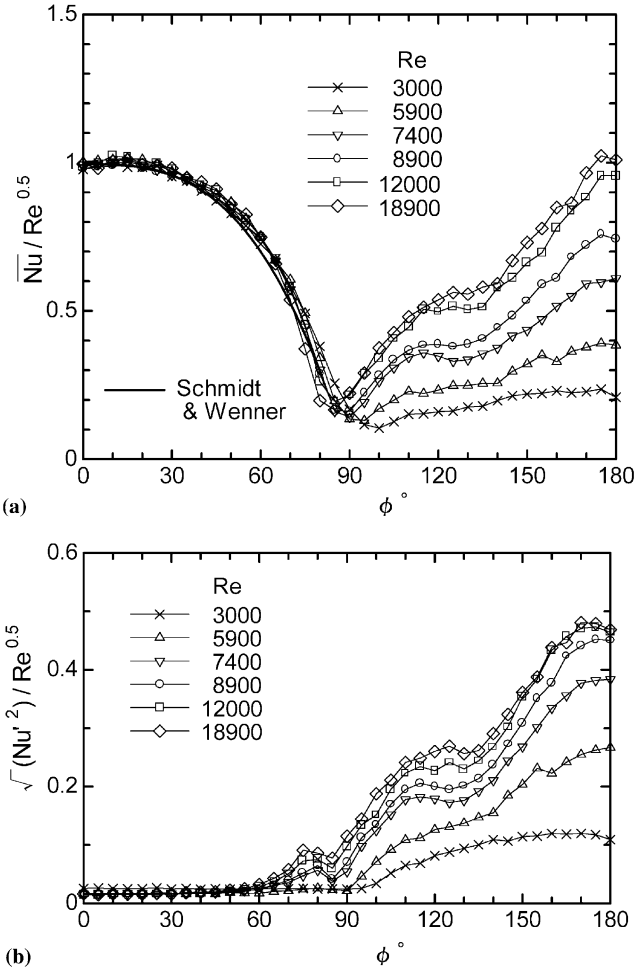

Fig. 4. Nusselt number distributions around a circular cylinder: (a) time-averaged Nusselt number and (b) fluctuating Nusselt number.

3.2. Fluctuating Nusselt number

Fig. 5(a) and (b) show time traces of the fluctuating Nusselt number and their power spectrums at various angular positions at $Re = 8900$ and 5900, respectively. At $Re = 8900$, the characteristics of the fluctuating Nusselt number are very similar to those at $Re \approx 20,000$ (Nakamura and Igarashi, 2002a). In the laminar flow region ($\phi = 70°$), the Nusselt number fluctuates periodically following the vortex shedding behind the cylinder, and a distinct peak exists in the power spectrum at the vortex shedding frequency f_s. This feature becomes prominent with an increase in the Reynolds number, as shown in Fig. 6(a), which is related to the shortening of the vortex formation length. At the rear of the cylinder ($\phi \geqslant 150°$) in Fig. 5(a), the power spectrum has a distinct peak at the vortex shedding frequency. In particular, the power spectrum at approximately $\phi = 180°$ has a peak at $2f_s$. This is caused by an alternating reattached flow caused by the alternating rolling-up of the shear layers that have separated from the cylinder (Igarashi,

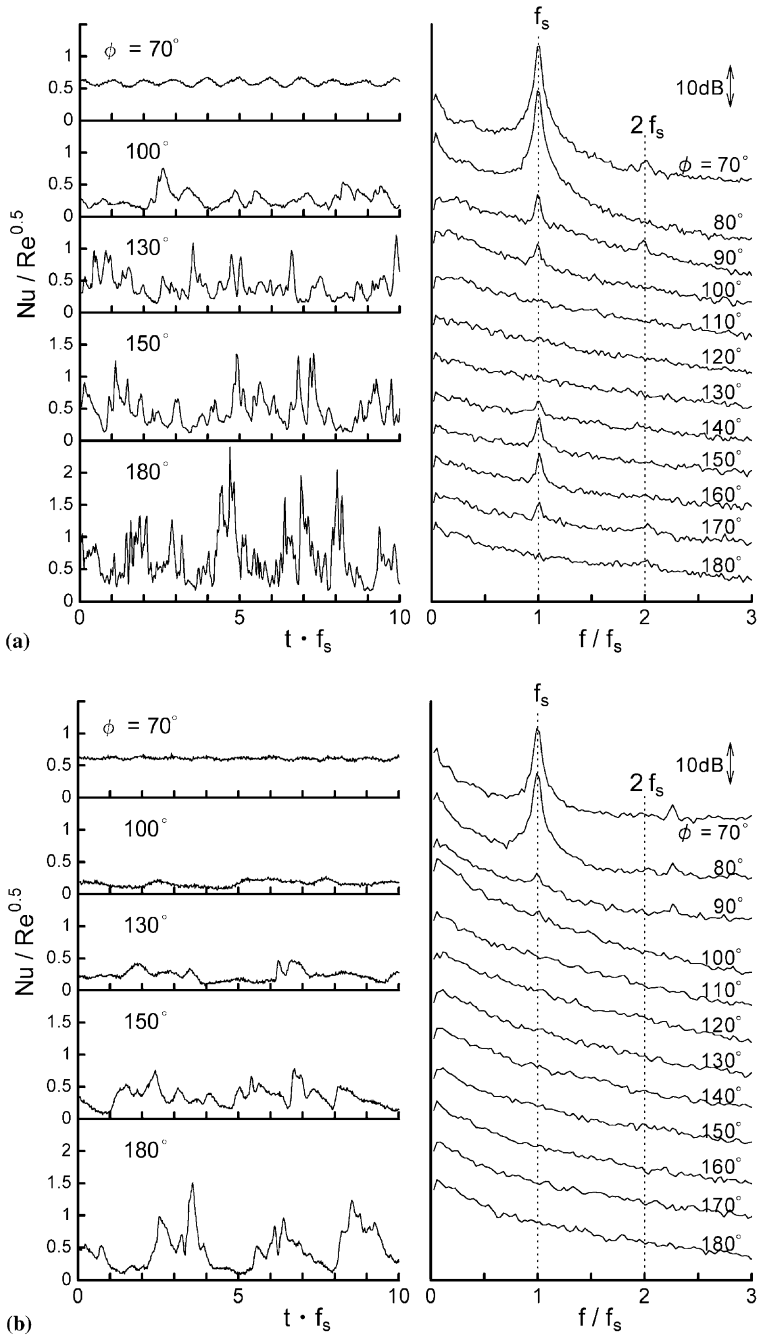

Fig. 5. Time traces of fluctuating Nusselt number and their power spectrums at various angular positions: (a) $Re = 8900$ and (b) $Re = 5900$.

1983; Nakamura and Igarashi, 2002a). The reattached reverse flow separates at around $\phi = 150°$. In the region in front of the flow reattached region ($110° \leqslant \phi \leqslant 130°$), no distinct peak appears in the power spectrum. This indicates that the surface flow in this region is not interlocked by the vortex shedding. In the region just behind the flow separation point ($90° \leqslant \phi \leqslant 100°$), a peak at f_s appears in the power spectrum due to an effect of the fluctuation of the separated shear layer.

In contrast, at $Re = 5900$ (Fig. 5(b)), the power spectrum has no distinct peak in the separated flow region, except a slight peak just behind the flow separation point. As shown in Fig. 6(b) and (c), the peak at $\phi = 150°$ and 180° disappear below $Re = 6000$ and 8000, respectively. This indicates that the alternating reattached flow at the rear of the cylinder initiates at approximately $Re = 6000$–8000. The formation of the reattached flow at the rear of the cylinder produces the plateau in the Nusselt number distributions ($110° \leqslant \phi \leqslant 130°$) in the range above $Re = 6000$–8000, as shown in Fig. 4. According to Igarashi (1983), a fluctuating pressure distribution around a circular cylinder has a

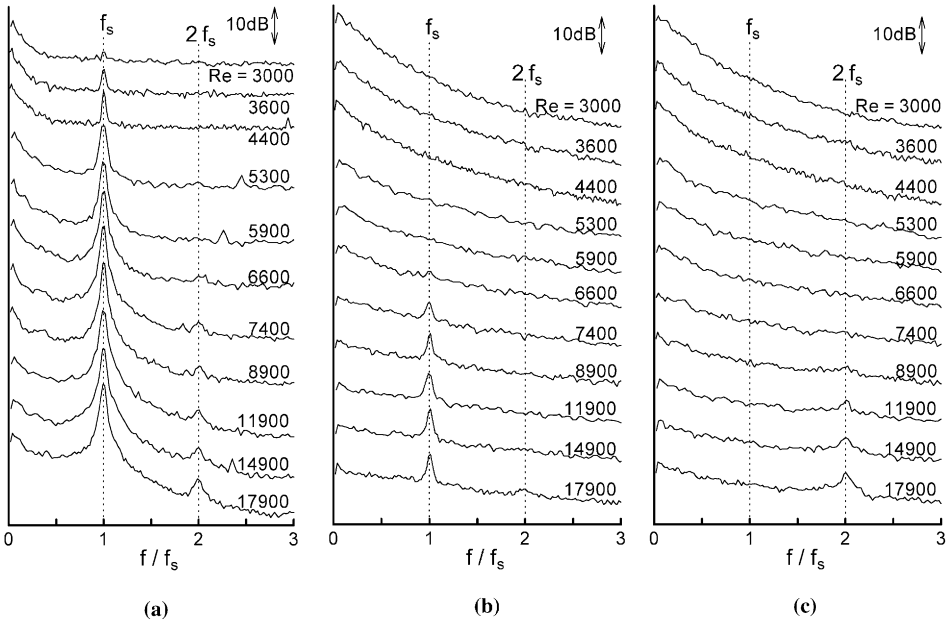

Fig. 6. Power spectrums of fluctuating Nusselt number for $Re = 3000$–$18,000$: (a) $\phi = 70°$, (b) $\phi = 150°$ and (c) $\phi = 180°$.

local maximum at $\phi = 155°$, at which the reattached reverse flow separates. This maximum disappears below $Re = 6000$–8000 (Norberg, 1993), corresponding to the range for which the reattached flow disappears.

4. Three-dimensional characteristics

4.1. Smoke visualization

Fig. 7 shows spanwise flow visualizations of the separated shear layer, obtained by the smoke-wire method. The test cylinder, which is positioned in the left side of each photograph, is 15 mm in diameter and 360 mm in length and has square end plates (150×150 mm). Only the opposite side of the shear layer is visualized by setting a constantan wire 0.1 mm in diameter at $x = -30$ mm and $y = 2$ mm, where x and y reflect the streamwise and cross-stream directions from the center of the cylinder, respectively. The separated shear layer rolls up and a reverse flow toward the rear of the cylinder is formed. At $Re = 2900$, the smoke entering the reverse flow does not reach the rear end of the cylinder due to the elongation of the shear layer. This leads to an inactive feature in the heat transfer at the rear of the cylinder, resulting in the decrease in both the time-averaged and fluctuating Nusselt numbers, as shown in Fig. 4(a) and (b). With the increase in the Reynolds-number, the smoke partly reaches the rear end ($Re = 4800$, 5800), with the forward movement of the vortex formation region. This suggests that the reattached flow initiates partially at around $Re = 5000$. At $Re = 7700$, the smoke in most of the axis reaches the rear end, corresponding to the appearance of the regularity in the fluctuating Nusselt number at the rear of the cylinder ($\phi \geqslant 150°$) for $Re > 6000$–8000. With the initiation of the reattached flow ($Re > 5000$–8000), both the time-averaged and fluctuating Nusselt numbers in the separated flow region increases suddenly, as shown in Figs. 1 and 4.

The flow visualization also indicates that the shear layer has a quasi-periodic spanwise nonuniformity, the wavelength of which is roughly one diameter throughout the Reynolds number range examined herein. This is likely caused by the formation of the streamwise vortices that originated from the "mode-B instability" (Williamson, 1996b), the existence of which has been observed for a wide range of Reynolds numbers ($Re = 330$–$21,000$) by Bays-Muchmore and Ahmed (1993).

4.2. Time-spatial characteristics

Fig. 8(a)–(c) show time-spatial characteristics of the heat transfer as measured by the infrared thermograph. The instantaneous distributions of the Nusselt number, $Nu/Re^{0.5}$, at the rear of the cylinder (top) and time histories of spanwise Nusselt number distribution at the rear stagnation line of $\phi = 180°$ (bottom) are shown. Although the fluctuation of the heat transfer for the infrared measurements was considerably attenuated due to the heat capacity on the cylinder surface, the time-spatial characteristics presented here produce valuable information. The instantaneous distribution shows a remarkable increase in Nusselt number with increasing Reynolds number at approximately $\phi = 180°$, due to the formation of the reattached flow. These distributions

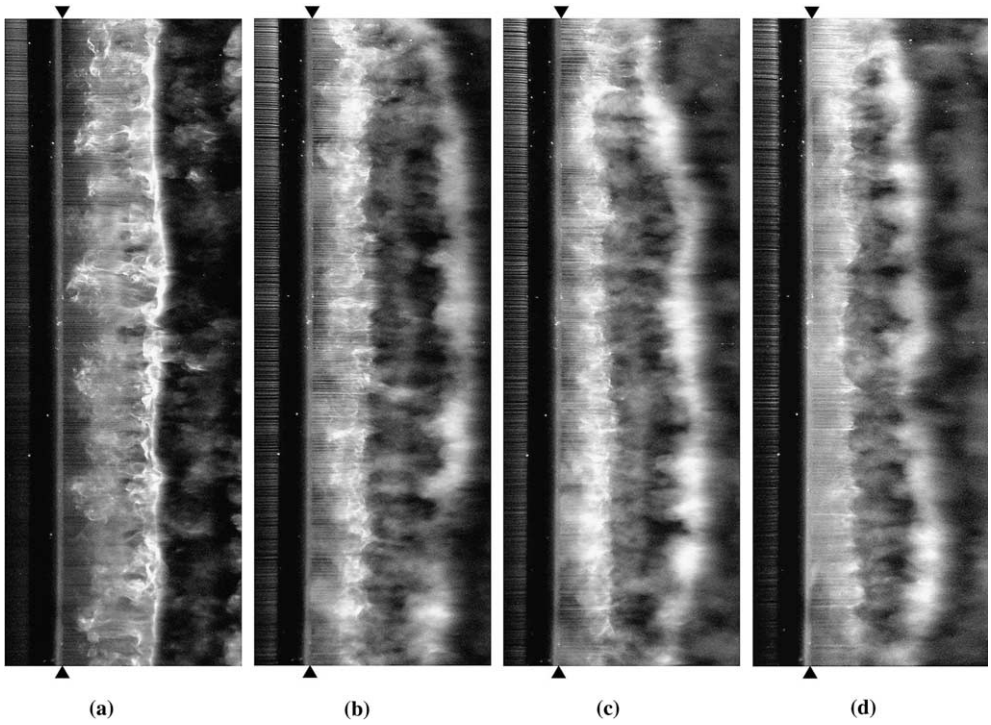

Fig. 7. Spanwise flow visualization of the separated shear layer; (▼) and (▲) indicate the rear end of the cylinder, the flow direction is from left to right: (a) $Re = 2900$, (b) $Re = 4800$, (c) $Re = 5800$ and (d) $Re = 7700$.

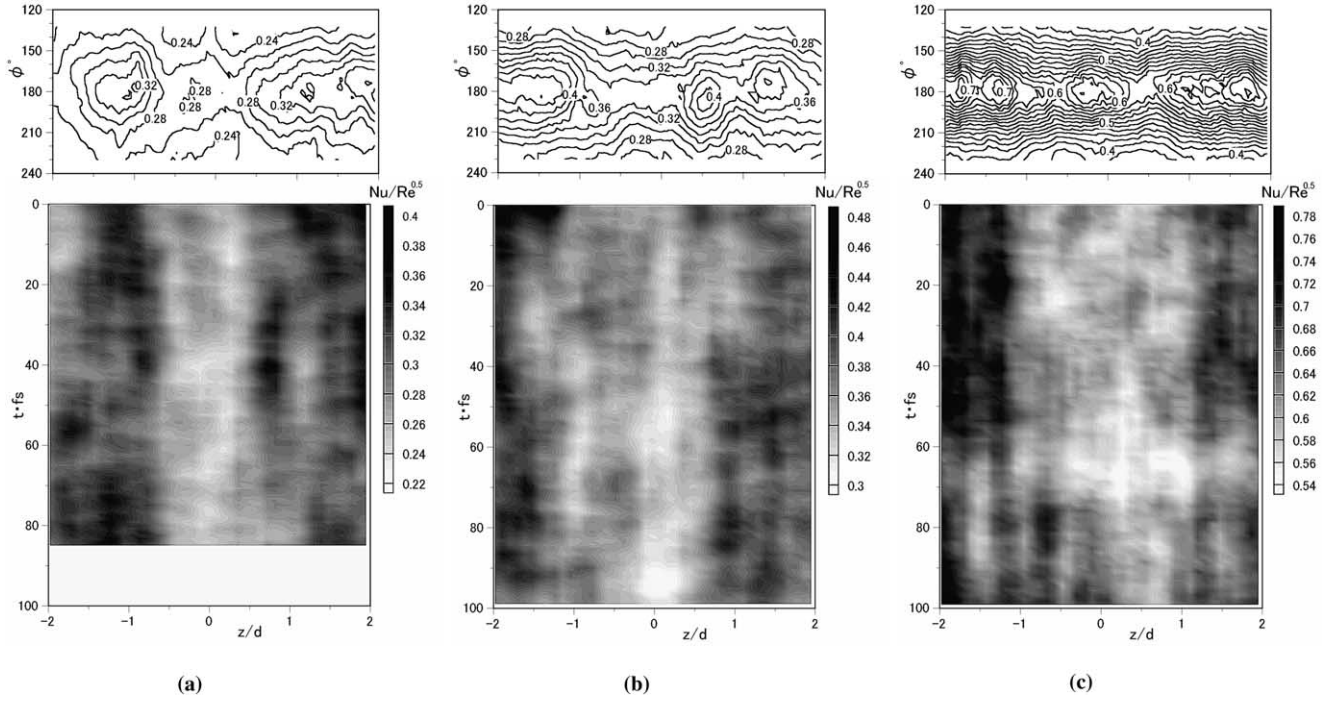

Fig. 8. Instantaneous distributions of Nusselt number, $Nu/Re^{0.5}$, at the rear of the cylinder (top) and time histories of spanwise Nusselt number distribution at $\phi = 180°$ (bottom): (a) $Re = 4800$, (b) $Re = 7200$ and (c) $Re = 9600$.

have a quasi-periodic spanwise nonuniformity, the wavelength of which is roughly one diameter throughout the Reynolds number range examined herein. This nonuniformity is reflected by the nonuniformity in the shear layers, as shown in Fig. 7, which originates from the streamwise vortices formed in the near-wake. As

indicated in the time histories at $\phi = 180°$, the spanwise nonuniformity in the Nusselt number is essentially steady for several tens shedding cycles. The above feature is probably related to the feedback mechanism in the formation of the streamwise vortices, as investigated by Williamson (1996b).

5. Conclusions

Unsteady heat transfer from a circular cylinder to the cross-flow of air was investigated experimentally for Reynolds numbers from 3000 to 15,000. The primary results are as follows:

1. The alternating reattached flow, which is caused by the rolling-up of the separated shear layers, is formed at the rear of the cylinder ($\phi \geqslant 150°$) in the range of $Re > 5000$–8000, due to the forward movement of the vortex formation region with increasing Reynolds number. With the initiation of the reattached flow, both time-averaged and fluctuating Nusselt numbers around the rear stagnation point increases suddenly.
2. The investigation of the time-spatial characteristics of the heat transfer in the separated flow region reveals the existence of spanwise nonuniformity, the wavelength of which is roughly one diameter. This nonuniformity is reflected by the nonuniformity in the shear layers, which originates from the streamwise vortices formed in the near-wake.

References

Bays-Muchmore, B., Ahmed, A., 1993. On streamwise vortices in turbulent wakes of cylinders. Phys. Fluids A 5 (2), 387–392.

Bloor, S.M., 1964. The transition to turbulence in the wake of a circular cylinder. J. Fluid Mech. 19, 290–304.

Boulos, M.I., Pei, D.C.T., 1974. Dynamics of heat transfer from cylinders in a turbulent air stream. Int. J. Heat Mass Transfer 17, 767–783.

Igarashi, T., 1983. Fluid flow and heat transfer in separated region of a circular cylinder. In: 4th ASME-JSME Thermal Eng. Joint Conf., Honolulu, Hawaii, vol. 3, pp. 87–93.

Igarashi, T., Hirata, M., 1977. Heat transfer in separated flows. Part 2: theoretical analysis. Heat Transfer Jpn. Res. 6 (3), 60–78.

Kumada, M., Ishihara, K., Kato, M., 1992. Unsteady characteristics of heat transfer on a separated region of a circular cylinder. In: 2nd JSME-KSME thermal Eng. Conf., Kitakyushu, Japan, vol. 2, pp. 37–42.

Nakamura, H., Igarashi, T., 2002a. Unsteady heat transfer in separated flow behind a circular cylinder. In: Taine, J. (Ed.), 12th Int. Heat Transfer Conf, vol. 2. Elsevier, pp. 729–734.

Nakamura, H., Igarashi, T., 2002b. Heat transfer in separated flow behind a circular cylinder for Reynolds numbers from 120 to 30,000 (1st Report, time-averaged characteristics). Trans. Jpn. Soc. Mech. Eng. 68 (675), 3122–3129 (in Japanese).

Nakamura, H., Igarashi, T., 2003. Heat transfer in separated flow behind a circular cylinder for Reynolds numbers from 120 to 30,000 (2nd Report, unsteady and three-dimensional characteristics). Trans. Jpn. Soc. Mech. Eng. 69 (681), 1224–1232 (in Japanese).

Norberg, C., 1993. Pressure forces on a circular cylinder in cross flow. In: Eckelmann, H., Graham, J.M.R., Huerre, P., Monkewitz, P.A. (Eds.), IUTAM Symp. Bluff-Body Wakes, Dynamics and Instabilities. Springer-Verlag, pp. 275–278.

Norberg, C., 2003. Fluctuating lift on a circular cylinder. Review and new measurements. J. Fluids Struct. 17, 57–96.

Peterka, J.A., Richardson, P.D., 1969. Effects of sound on separated flows. J. Fluid Mech. 37, 265–287.

Prasad, A., Williamson, C.H.K., 1997. Three-dimensional effects in turbulent bluff-body wakes. J. Fluid Mech. 343, 235–265.

Richardson, P.D., 1963. Heat and mass transfer in turbulent separated flows. Chem. Eng. Sci. 18, 149–155.

Roshko, A., 1993. Perspectives on bluff body aerodynamics. J. Wind Eng. Ind. Aerodyn. 49, 79–100.

Schiller, V.L., Linke, W., 1933. Druck- und Reibungswiderstand des Zylinders bei Reynoldsschen Zahlen 5000 bis 40,000. Z. Flugtechnik Motorluftschiffahrt 24 (7), 193–198.

Schmidt, E., Wenner, K., 1941. Wärmeabgabe uber den Umfang eines angeblasenen geheizten Zylinders. Forschung 12, 65–73.

Scholten, J.W., Murray, D.B., 1998. Unsteady heat transfer and velocity of a cylinder in cross flow. 1. Low freestream turbulence. Int. J. Heat Mass Transfer 41, 1139–1148.

Williamson, C.H.K., 1996a. Vortex dynamics in the cylinder wake. Annu. Rev. Fluid Mech. 28, 477–539.

Williamson, C.H.K., 1996b. Three-dimensional wake transition. J. Fluid Mech. 328, 345–407.